

A comparison of two schemes for the convective transport of chemical species in a Lagrangian global chemistry model

By W. J. COLLINS^{1*}, R. G. DERWENT¹, C. E. JOHNSON¹ and D. S. STEVENSON²

¹*Met Office, UK*

²*Edinburgh University, UK*

(Received 9 March 2001; revised 19 September 2001)

SUMMARY

We have developed a detailed parametrization scheme to represent the effects of subgrid-scale convective transport in a three-dimensional chemistry-transport model (CTM). The CTM utilizes the meteorological fields generated by a general-circulation model (GCM) to redistribute over 70 chemical species. The convective transport is implemented using the convective mass fluxes, entrainment rates and detrainment rates from the GCM.

We compare the modelled distributions of ²²²Rn with observations. This shows that the vertical profile of this species is affected by the choice of convective-transport parametrization. The new parametrization is found to improve significantly the simulation of ²²²Rn over the summertime continents.

KEYWORDS: Chemistry-transport model Convection Radon

1. INTRODUCTION

In recent years many three-dimensional global tropospheric chemistry models have been developed that have started to show success in simulating the chemical evolution of the troposphere (Kanakidou *et al.* 1999a,b). These models describe the emission of trace gases, their transport and their chemical reactions with varying degrees of sophistication and elaboration. Although there are some emission sources in the free troposphere, such as aircraft and lightning, the majority of emissions come from surface sources whether man-made, such as fossil-fuel burning, or from natural sources, such as vegetation or soils. The accuracy with which chemistry models can simulate the distribution of the trace gases and their reaction products depends on their ability to represent the transport of the chemical species out of the boundary layer, where they are emitted, and into the free troposphere. In the free troposphere, species are more susceptible to long-range transport due to stronger winds and fewer removal processes. The chemical regimes are very different in the polluted boundary layer compared with the cleaner free troposphere. Lin *et al.* (1988) showed that the efficiency of ozone production from NO_x, was much higher in less polluted regions of the atmosphere, and Pickering *et al.* (1992) showed that lifting polluted air into the free troposphere greatly increased the ozone produced from biomass-burning emissions.

Many studies have shown that convection is an extremely important transport process for tropospheric chemistry, providing an efficient mechanism for removing pollutants from the boundary layer and lifting them to higher altitudes (e.g. Gidel 1983). Vertical velocities in large convective clouds can reach 10 m s⁻¹, and so can easily lift material from the boundary layer to the upper troposphere in a few tens of minutes. This should be contrasted with timescales of the order of weeks or months for adiabatic processes and turbulent diffusion to achieve the same effect. Thompson *et al.* (1994) showed that a large fraction of the CO emitted into the boundary layer of the USA was vented to the free troposphere by deep convective processes over the centre of the continent. The vertical transport of CO and other ozone precursors can lead to enhanced

* Corresponding author: Climate Research Division, Met Office, London Road, Bracknell, Berkshire RG12 2SZ, UK. e-mail: bill.collins@metoffice.com

ozone production in the upper troposphere, a region where ozone is most effective as a radiatively active gas (Lacis *et al.* 1990). Convective clouds can also bring down lower-stratospheric ozone into the upper-tropospheric region. Recent studies show that the upper troposphere is more photochemically active than previously thought, due to the convective transport of radical precursors, such as hydroperoxides and carbonyls (Jaeglé *et al.* 1997; Prather and Jacob 1997; Collins *et al.* 1999).

Convective clouds have a horizontal extent of the order of 1 km, and the extent of the updraught can be significantly less than this. The horizontal grid spacing of the latest global chemistry-transport models varies from 1.9° (Lawrence *et al.* 1999) to 10° (Berntsen and Isaksen 1997). These equate to ~ 200 – 1000 km, and so global chemistry models are unable to resolve convective process. Instead, models have to parametrize these subgrid-scale effects. Two methods for parametrizing the effects of subgrid-scale convection in a global chemistry-transport model (STOCHEM) are described in this paper.

As well as transporting material, convective clouds have other important effects on tropospheric chemistry. Soluble chemical species in the cloud, such as nitric acid and hydrogen peroxide, are scavenged by precipitation and so are not transported upwards as efficiently as insoluble species (Mari *et al.* 2000). Deep convection can generate lightning flashes which produce large quantities of NO in the free troposphere (Price *et al.* 1997). The cirrus anvils of cumulonimbus will reflect solar radiation upwards, hence decreasing the chemical photolytic reaction rates below the anvil and increasing them above (e.g. Madronich 1987). These processes are not discussed in this paper. Details of their implementation in the STOCHEM model can be found in papers by Collins *et al.* (1997, 1999).

2. MODEL DESCRIPTION

The transport model used for this study (STOCHEM) has been developed to simulate tropospheric chemistry with 70 chemical species and around two hundred chemical and photochemical reactions (Collins *et al.* 1997, 1999; Stevenson *et al.* 1998a).

Most global transport models are Eulerian. In that approach, a regular rectangular grid is built throughout the model domain and a finite-differencing scheme is used to describe the processes involved in this fixed framework. The accurate representation of the advection of trace gases is not straightforward if negative concentrations, numerical dispersion and short time steps are to be avoided (Chock and Winkler 1994; Dabdub and Seinfeld 1994). Pseudo-spectral techniques offer a formally accurate alternative to the conventional finite-difference approach in models of atmospheric dynamics. However, when applied to atmospheric trace-gas transport, they may generate negative concentrations and spurious oscillations (Thuburn and McIntyre 1997). In this study, a Lagrangian approach has been adopted using 50 000 constant-mass parcels of air carrying the mixing ratios of chemical species. The centroids of these parcels are advected by interpolated winds from the Met Office global general-circulation model (GCM) (Cullen 1993), called the Unified Model (UM). One advantage of Lagrangian advection is that all trace-gas species are advected together, so the chemistry and transport processes can be uncoupled and chemistry time steps determined locally. There also are disadvantages with the Lagrangian approach; species concentrations are defined on parcel centroids but output is generally required on an Eulerian grid. This may be over- or underdetermined in a practical implementation where the number of parcels may be limited. Distortions due to wind shears can render the notion of a distinct air

parcel meaningless, but mixing can be considered equivalent to redefining the air parcels (Walton *et al.* 1988).

(a) *Advection scheme*

The vertical coordinate in the UM is a hybrid η coordinate. Near the surface η is terrain-following and is equal to P/P_s (where P is the pressure and P_s is the surface pressure); at heights where pressures are lower than 30 hPa, η follows the pressure surfaces and is equal to $P/(1000 \text{ hPa})$.

The Lagrangian parcels are advected according to six-hourly winds taken from a climate version of the UM (Johns *et al.* 1997), which are based on a grid of 3.75° longitude \times 2.5° latitude and 19 unevenly spaced η levels between 0.997 and 0.0046 for the horizontal winds (v_U and v_V) and between 0.994 and 0.01 for the vertical wind (v_W). There are three levels below $\eta = 0.9$ (~ 900 hPa).

The chemistry-transport model can be run in two modes, on-line in which the chemistry code is called as a subroutine of the driving GCM, or off-line in which the GCM is run first, all the meteorological variables needed are archived and the chemistry model is then run off the archive. In either case the GCM is run specifically to provide data for the chemistry model so that all the necessary diagnostic variables can be provided.

In this transport model, a Runge–Kutta fourth-order advection scheme is used. The velocities are obtained at the parcel positions and times by linear interpolation in the horizontal and in time. In the vertical dimension, the resolution is not sufficient to resolve the tropopause and a cubic interpolation is found to represent the curvature in the meteorological fields more accurately. Rigid boundaries are imposed at $\eta = 1$ (surface) and $\eta = 0.1$ (~ 100 hPa). Parcels that would be advected through these boundaries are forced to remain on them, although still influenced by horizontal winds, until advected into the model domain by a change in vertical wind.

By design, a Lagrangian scheme is always stable and any time step can be used within reason. Increasing the time step just increases the error in the trajectory. This contrasts with an Eulerian advection scheme which becomes unstable if the time step exceeds the Courant–Friedrichs–Levy criterion that $\Delta t < \Delta L/v$ where ΔL is the grid spacing and v is the wind speed, i.e. the condition that air must travel less than one grid length in one time step. Methven (1997) showed that errors in Lagrangian trajectories did not increase significantly until the advection time step approached the time resolution of the wind data. The wind data available have a six-hourly resolution so an advection time step (Δt) of three hours was used.

Doty and Perky (1993) found that, for a mesoscale simulation of an Atlantic storm, one-hourly data resolution was necessary, but they suggested that this was largely to resolve the rapidly varying vertical motions in the storm. Lee *et al.* (1997) suggested that degrading the resolution in the horizontal reduced the sensitivity of the trajectories to the temporal resolution, and vice versa.

(b) *Subgrid-scale mixing*

As the meteorological data available necessarily have finite resolution, some account has to be taken of important processes that occur on scales too small to be resolved by the data. Those influencing transport the most are diffusion (the parametrization of subgrid-scale eddy transport) and convection (vertical motions often associated with clouds, occurring on a subgrid-scale in the horizontal, but possibly extending across several model layers in the vertical).

A Lagrangian transport scheme differs from an Eulerian one in that it does not suffer from excessive numerical diffusion. In fact, instead of having to avoid diffusion, diffusion needs to be added. Without diffusive mixing between air parcels, the species concentrations on the parcels can become more and more extreme, as some pick up emissions and others do not. This can lead to excessively noisy concentration fields, which are obviously unrealistic since diffusive processes prohibit the creation of sharp concentration gradients and air parcels do not maintain their integrity indefinitely. To parametrize the mixing of air parcels, the species concentrations χ on each parcel are relaxed towards an Eulerian background concentration $\bar{\chi}$ by adding a term $d(\bar{\chi} - \chi)$ every time step, where d is a coefficient varying between 0 and 1 determining the extent of the mixing. The background is calculated from the average concentration of all the parcels within an Eulerian grid volume, where the grid used is a regular $72 \times 36 \times 9$ in longitude, latitude and the vertical, giving an average parcel occupancy of two per grid volume (more near the equator, less near the poles). The nine vertical levels are evenly spaced in η ($\Delta\eta = 0.1$). Constant η spacing is approximately equivalent to constant pressure spacing, which means the layers are approximately of equal mass and, hence, contain roughly equal numbers of parcels. The coefficient d can be related to the horizontal eddy diffusion K_H (Walton *et al.* 1988) by

$$d = \left(1 - \frac{\sigma_0^2}{\sigma_0^2 + 2K_H\Delta t} \right)$$

where σ_0 is the characteristic horizontal extent of an air parcel (~ 300 km in this case). With a K_H of $1300 \text{ m}^2\text{s}^{-1}$ this would give $d = 0.3 \times 10^{-3}$. We therefore set d to 10^{-3} below $\eta = 0.3$ (~ 300 hPa) and to 10^{-6} above to reflect the reduction in mixing in the upper troposphere and lower stratosphere. We found that, in the troposphere, the results are relatively insensitive to the value of d in that varying the lower-troposphere value from 10^{-4} to 10^{-2} produced negligible change in monthly-mean distributions of chemical species. However, high values of d caused too much vertical mixing across the tropopause. The interparcel exchange process can be regarded as partial mixing between parcels caused by deformation and shear, or as a partial re-initialization of the parcel concentrations with background values each time step. The mixing has been parametrized so that it still conserves species mass. The interparcel mixing smooths out differences between individual parcels and the background, but does not diffuse the background (Eulerian average) concentrations.

Following Walton *et al.* (1998), we split the diffusion term into two parts

$$\frac{\partial \chi}{\partial t} = \nabla \cdot (\mathbf{K} \cdot \nabla \chi) = \nabla \cdot (\mathbf{K} \cdot \nabla \bar{\chi}) + \nabla \cdot (\mathbf{K} \cdot \nabla (\chi - \bar{\chi}))$$

where $\bar{\chi}$ is the Eulerian average concentration. The last term on the right-hand side is parametrized by the interparcel mixing. The first term on the right-hand side is accounted for by adding random displacements to the parcel each time step:

$$\mathbf{X} = \mathbf{X} + \mathbf{n}\sqrt{2\mathbf{K}\Delta t}$$

where \mathbf{X} is the parcel position, \mathbf{n} is a vector of normally distributed random numbers with zero mean and unit width. The horizontal diffusivity K_H is as above and the vertical diffusivity K_η is set to be $7 \times 10^{-11} \text{ s}^{-1}$. The vertical diffusivity corresponds to a K_z of around $10^{-2} \text{ m}^2\text{s}^{-1}$.

(c) *Boundary-layer parametrization*

As indicated by Stevenson *et al.* (1998a), parcels within the boundary layer are randomly assigned a vertical coordinate between the ground and a height slightly above the boundary-layer top because the boundary-layer mixing timescale is less than our advection time step. The extra height was added to simulate detrainment from the boundary layer. There is no explicit entrainment process modelled, except that due to the time variation of the height of the boundary-layer top. The depth of the boundary layer is produced as a diagnostic by the GCM where it is defined as the first level where the moist Richardson number exceeds 1.0 (Smith 1990).

(d) *The STOCHEM convection schemes*

Convection occurs on too small a horizontal scale (a few kilometres) to be resolved with our vertical wind field and so has to be parametrized. The original convection scheme in STOCHEM was basically diffusive in that it completely mixed air between the convective cloud top and the ground. The strength of the convection was based on the convective precipitation rate using a factor tuned to give comparable results to the UM (Stevenson *et al.* 1998a). The scheme ensured that the model simulated reasonably realistic chemical concentrations in the upper troposphere, enabling the model to be used to simulate the effect of aircraft emissions and the effects of climate change (Stevenson *et al.* 1997, 1998a, 1988b; Collins *et al.* 1999). One defect of the old diffusive scheme was that it excessively smeared out any vertical gradients in species concentrations. This was most noticeable in the ozone profiles in the upper troposphere. A technical point is that the old scheme, being Eulerian, broke the continuity of the Lagrangian trajectories. Parcel concentrations were effectively reset after undergoing convection.

We decided to utilize the convective diagnostics that had recently become available from the UM to make our parametrization of convection more physically based. At the same time we decided to implement the convective transport in a Lagrangian sense. We treat this transport in a probabilistic sense, with probabilities determined from the convective mass fluxes. Our Lagrangian parcels are so large that no one convective system can transport a whole parcel intact (about 100 billion tonnes each if we use 50 000 parcels). So, in reality, parcels will lose their identity during convective events. However, the convective scheme in the driving GCM is highly parametrized since it treats all the convective systems within a grid square ($3.75^\circ \times 2.5^\circ$) as a single convective ensemble. The mass fluxes in these ensembles are of the order of 10^{11} tonnes per three-hour advection time step, which is roughly equal to the mass of one parcel. While one parcel is not sufficient to characterize the entrainment and detrainment profiles of a convective ensemble, the average effect over many grid squares and many time steps will be to represent statistically the effect of convection on the vertical redistribution of chemical species.

The convection scheme in the UM is a mass-flux scheme with an instability closure (Gregory *et al.* 1997). It uses a bulk entraining single-cloud model, but simulates a range of cloud depths by forcing some detrainment at heights below the cloud top. It has self-consistent mass, entrainment and detrainment fluxes. While the UM scheme calculates both updraughts and downdraughts, only the updraughts have been implemented in STOCHEM. Downdraughts typically have around one tenth of the mass flux of the updraughts. The updraught and downdraught schemes are separately non-divergent, so one can be applied without the other with no inconsistency.

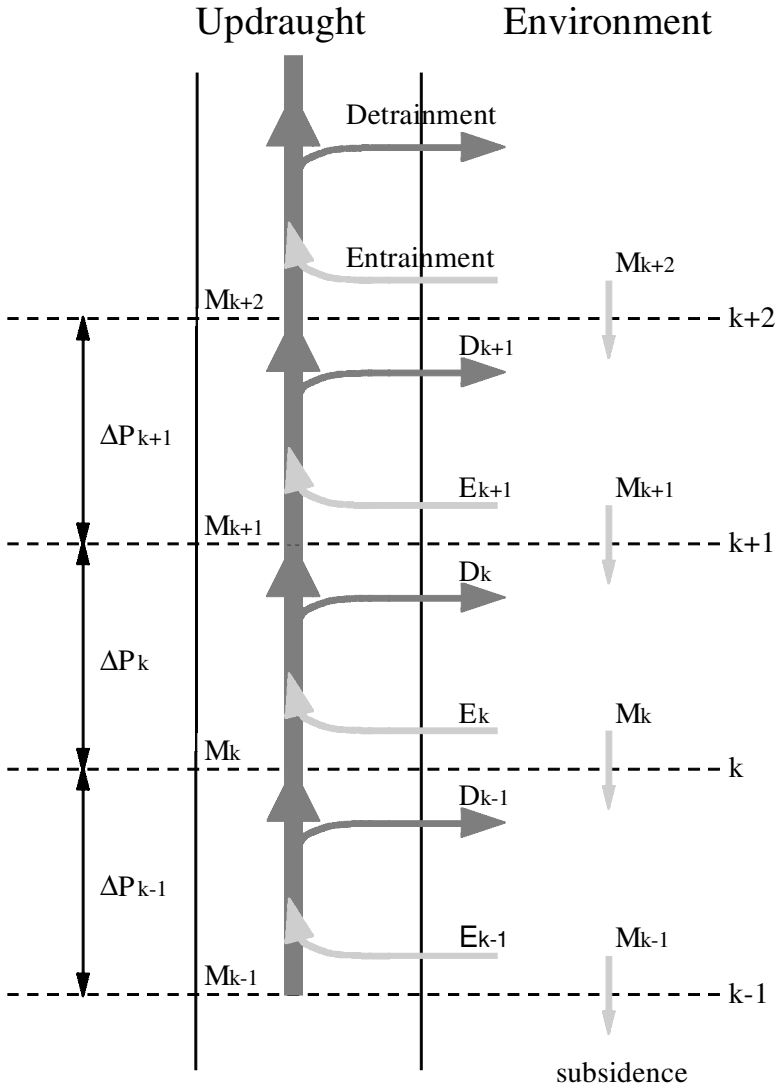


Figure 1. Schematic showing the fluxes used in the Unified Model’s convection scheme. Symbols are defined in the text.

The mass fluxes at each level are related to the entrainment and detrainment fluxes by:

$$M_{k+1} = M_k + E_k + D_k$$

where M_k and M_{k+1} are the updraught mass fluxes at levels k and $k + 1$, and E_k and D_k are the entrainment and detrainment fluxes at level k . All fluxes are in units of Pa s^{-1} . The fluxes are shown schematically in Fig. 1. Detrainment accounts both for detrainment of cloud air through turbulent mixing at the edge of the cloud and forced detrainment. Detrainment fluxes are defined as into the plume and hence are negative numbers. If the updraughts extend above the STOCHEM model top (currently 100 hPa) then they are forced to detrain completely in the level below the model top.

The UM convection scheme generates mass fluxes. We treat the mass fluxes as the rates of exchanging masses of air between the updraught and the environment. For the subsiding air, we convert from mass fluxes to velocities by making the assumption that the air over the whole grid square is descending.

For a parcel in level k , the probability (ϵ_k) of it being entrained into the updraught plume in a time step (Δt) is given by:

$$\epsilon_k = \Delta t \frac{E_k}{\Delta P_k}$$

where ΔP_k is the depth of the level in Pa. This probability is just derived from the residence time of a parcel in the environment at a particular level and is independent of the fraction of the grid square covered by the cloud. Once the parcel is in the plume, the probability of it detraining in level l (δ_{lk}) is given by the fraction of the plume detraining at that level multiplied by the probability of the parcel not having been detrained at an earlier level

$$\delta_{lk} = \frac{-D_l}{M_l} \left(1 - \sum_{l'=k+1}^{l-1} \delta_{l'k} \right).$$

This has the property that the sum of the detrainment probabilities from level k up to the cloud top is equal to one, i.e. all the parcels are forced to detrain from the plume in one time step. This is equivalent to assuming that the updraught velocities are sufficient for a parcel to ascend to the cloud top in less than a model time step.

To balance the updraught, parcels in the environmental air have to subside. The rate at which they need to do this is given by balancing the flux out of the environment at level k and the flux into the environment. This implies that the subsidence flux is equal to the updraught flux. To implement this, every parcel, whether it has undergone transport in the updraught or not, is moved downwards by an amount $M\Delta t$ (in Pa), where M is the mass flux interpolated to the parcel height. Figure 2 shows a simple example of the convection scheme. The mass fluxes are shown on the left-hand side. The entrainment and detrainment fluxes are combinations of step functions, whereas the updraught flux is continuous. In this example the entrainment flux is 50 hPa per time step between 1000 and 900 hPa, giving an entrainment probability of 0.5 per time step, hence, on average, half the parcels within this interval are transported upwards. Since the detrainment flux is constant between 500 and 400 hPa, the parcels are detrained evenly over this interval. All parcels then subside a distance given by the updraught flux.

The time step used in the GCM is 15 min for both the dynamics and the physics, with diagnostics output every six hours. As a compromise between these values, we have an advection time step in STOCHEM of three hours. If this were applied to our convection scheme, we would get mass fluxes at each level that were greater than the mass of air in the level. We, therefore, use the 15 min time step used in the GCM to run the convection scheme 12 times between each advection step.

The same GCM convection scheme is used to drive the old diffusive convective transport parametrization and the new Lagrangian-type one described here. The improvements are due to the extra diagnostic information that has become available.

(e) Computation

The chemistry-transport model has been optimized to run on a massively parallel computer, a Cray T3E. As a compromise between minimizing the run time and minimizing the inter-processor communication, we usually run on 36 processors. In the case

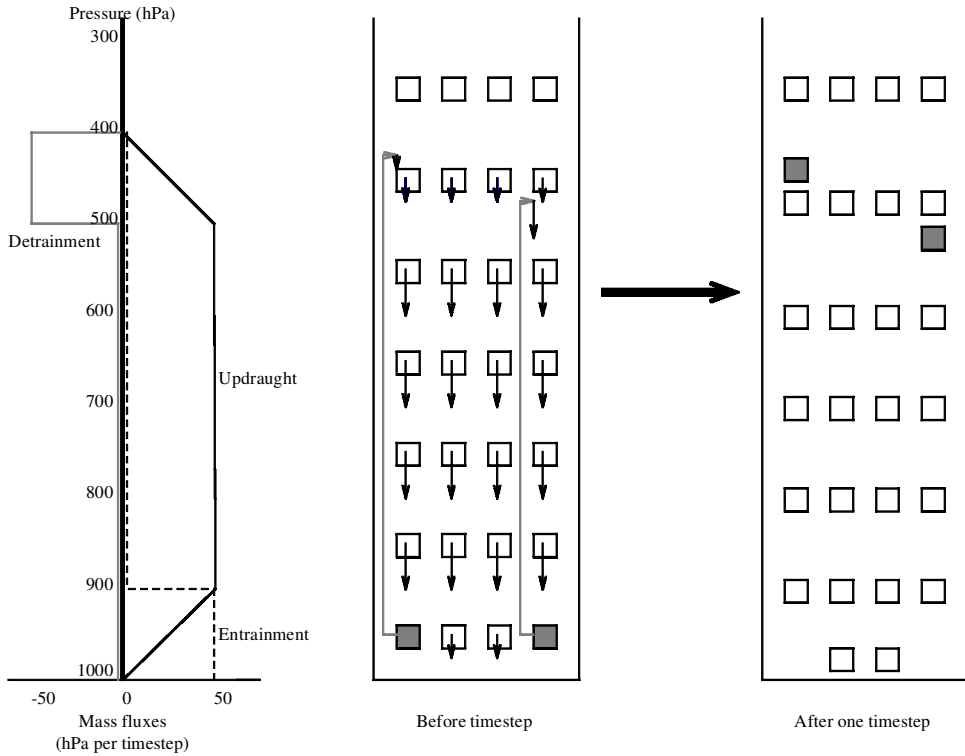


Figure 2. Schematic showing an example of the effect of the convection scheme on the location of air parcels. In this case, half of the parcels between 1000 and 900 hPa (shaded) are lifted to heights between 500 and 400 hPa.

of a 36-processor run we divide the globe into nine latitude bands of 20° , each of which is divided into a number of longitude sections, varying from one to six, such that each section covers a roughly equal surface area of the globe. Each processor computes all the physical processes (such as advection, convection, wet and dry deposition) for one section of the globe.

When simulating the full tropospheric chemistry, the most expensive section of the code is the integration of the differential equations specifying the chemical reactions. This takes about 60% of the central-processor-unit (CPU) time for the chemistry model, so it is important that the computational load is balanced as evenly as possible. An imbalance occurs because the geographical division between processors is not exact, with some processors covering a slightly larger area of the globe, and hence more air parcels, than others. These processors pass the information on their extra air parcels to processors covering fewer parcels so that each processor integrates the chemical reactions on exactly the same number of parcels.

The CPU time taken is about 12 hours per processor to simulate one year of tropospheric chemistry. To run with just ^{222}Rn for the experiments in this paper takes half this time. We have not removed the chemical load-balancing scheme even though, with the very simple chemistry used, the extra communication overhead is as great as the efficiency saving.

3. EXPERIMENTS

As discussed previously, our model has been designed to simulate many of the complex series of reactions involved in tropospheric chemistry, with a focus on the degradation of hydrocarbons and the production of ozone. However, to try to understand the effect of transport processes in the model it is often easier to study species with much simpler chemistry. Following Jacob and Prather (1990) amongst others, we focus in this paper mainly on the distribution of ^{222}Rn whose sole loss process is radioactive decay with an e-folding lifetime of 5.5 days. This is of the same order as the timescale for convective ventilation of the planetary boundary layer, although Penner *et al.* (1998) have shown that a better test of a model convection scheme would be to use a tracer with a lifetime of around one day.

Our emissions are the same as those stipulated for the World Climate Research Programme workshop on scavenging and deposition processes (Rasch *et al.* 2000). We specify the ^{222}Rn source strength to be $1.0 \text{ atom cm}^{-2}\text{s}^{-1}$ over land areas between 60°N and 60°S . To account for partially frozen land, the source strength is reduced to $0.5 \text{ atom cm}^{-2}\text{s}^{-1}$ over land areas between 60°N and 70°N , with no seasonal variation. Land areas north of 70°N , south of 60°S and the whole of Greenland are assumed to be permanently frozen and to be a zero source of ^{222}Rn . This gives a global source strength of around 15 kg per year. Jacob and Prather (1990) suggested that source strengths can vary locally by up to a factor of three, depending on soil type and season. However, there are insufficient data to incorporate this variability into global models. Uncertainty in emissions may cause problems when comparing model results with surface measurements in cases where local emissions provide the dominant contribution to the radon concentrations.

The radon emissions are added on a $5^\circ \times 5^\circ$ grid-square basis. The emissions for each grid square are distributed equally over all the parcels that are within the boundary layer in that grid square. If there are no cells within the boundary layer for a particular grid square then the emissions are stored until a parcel does pass through.

For this paper, the model is run off-line, taking the driving meteorology from a climate integration of the GCM. It uses a 1990s radiative forcing, but the meteorology does not correspond to any particular calendar year.

4. RESULTS

The main features of the radon distributions can be seen in Figs. 3 and 4. These show results for the model with no convection, the old diffusive convection scheme and the new Lagrangian convection scheme. The results are averaged over the month of June.

Figures 3(a)–(c) show a slice from the North Pole to the South Pole along a line of longitude at 22.5°E for each scheme. The peaks at around 35°N – 65°N and 30°S – 25°N are located over Europe and Africa, respectively. Figures 3(d)–(f) show a slice around the globe along a line of latitude at 2.5°N for each scheme. The peaks at around 80°W – 60°W , 10°E – 40°E and 100°E – 120°E are located over South America, Africa and south-east Asia, respectively. These figures show clearly that the effect of convection is to smear out vertically the concentrations in the plumes, so reducing the vertical gradients. It is noticeable that the two convection schemes have similar effects on the radon distribution, even though they use very different approaches. One difference is that the Lagrangian scheme has a greater tendency than the diffusive one to leave isolated pockets of high radon concentrations in the upper troposphere.

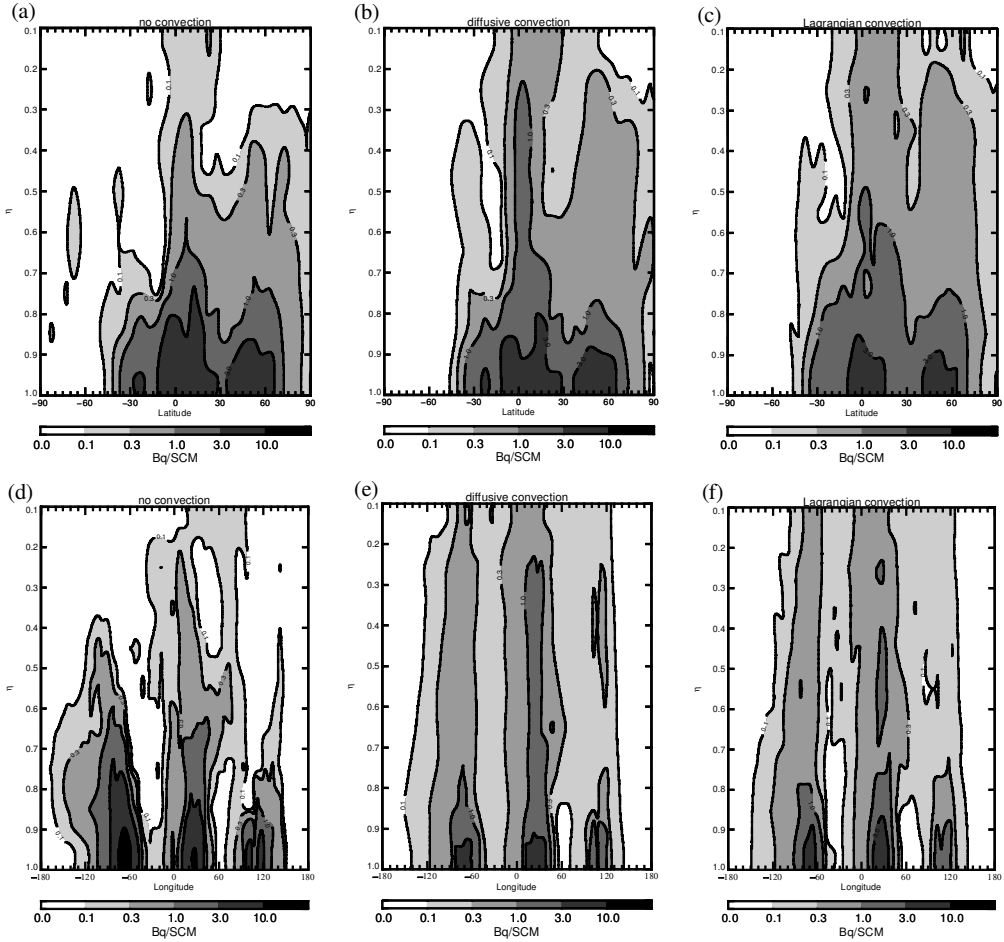


Figure 3. Slices through the June ^{222}Rn concentrations (in Bq per standard cubic metre (SCM)) for the three different convection schemes (see text). Panels (a), (b) and (c) show slices around a line of longitude (22.5°E), and panels (d), (e) and (f) show slices around a line of latitude (2.5°N). The vertical coordinate (p) is approximately pressure/1000 hPa.

In the latitude–longitude plots (Fig. 4) the surface radon is highest over the continents and lowest over the oceans. Since the ^{222}Rn lifetime is so short, there is little advection out from the continents. The two transport schemes with convection are similar, both showing lower concentrations than the case with no convection, especially in the tropics. This reflects the lifting of radon-rich air out of the boundary layer. In the mid troposphere (~ 650 hPa) the concentrations are nearly an order of magnitude less than at the surface. They again generally follow the continents, however with more advection out over the oceans than was found at the surface. The two convection schemes show broadly similar results with decreased radon concentrations over the ITCZ and generally increased concentrations over the continents. The concentrations are slightly higher in the Lagrangian scheme. In the upper troposphere (~ 350 hPa) concentrations are lower still. The contours no longer follow the outline of the continents but appear as localized maxima. In the two schemes with convective transport there are higher radon concentrations almost everywhere, with particularly large increases over convective centres in

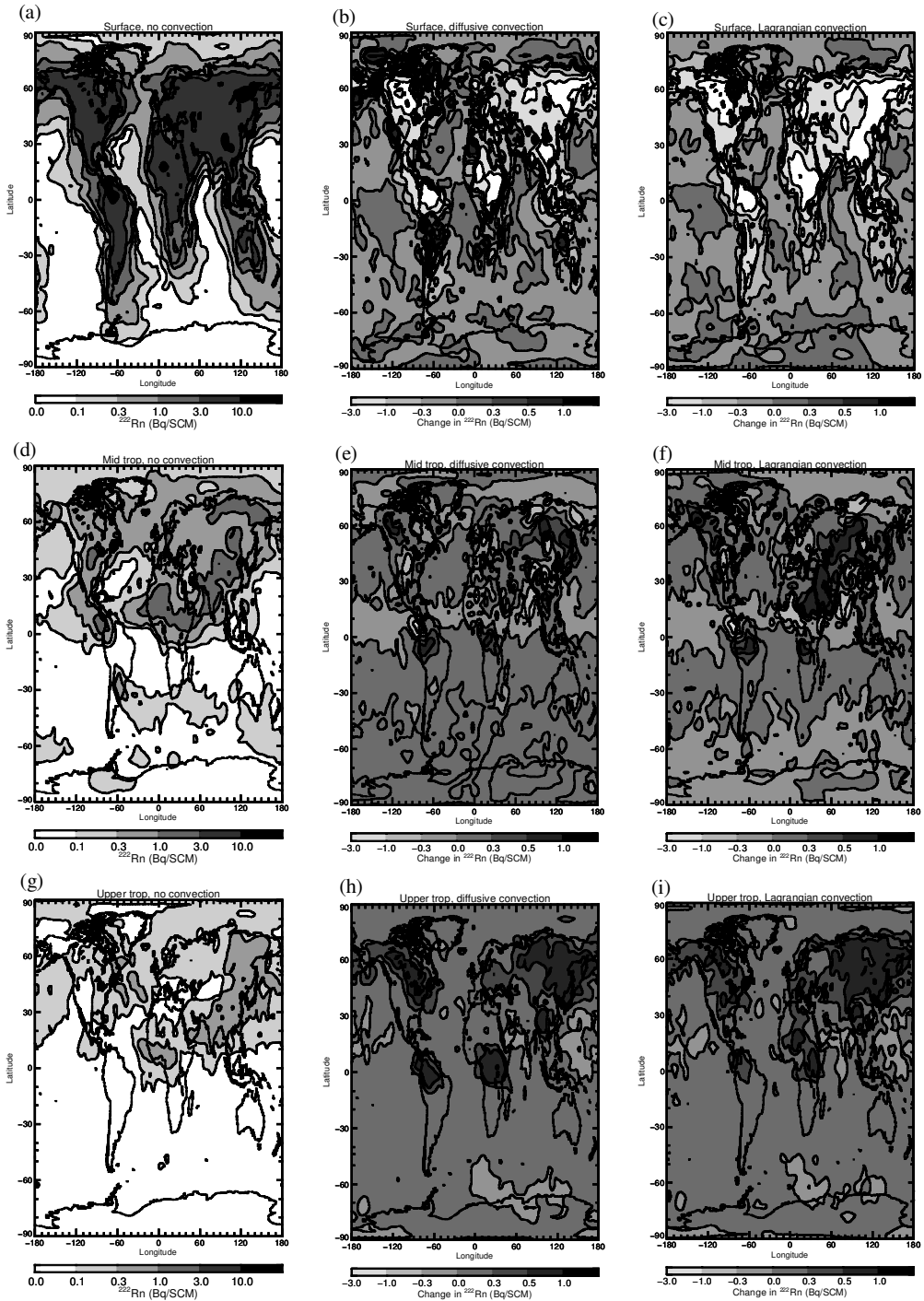


Figure 4. June ^{222}Rn concentrations (in Bq per standard cubic metre (SCM)) at three vertical levels (surface, mid troposphere, and upper troposphere—see text) for the three different convection schemes. Panels (a), (d) and (g) show the absolute concentrations with no convection scheme applied. Panels (b), (e) and (h) show the concentration difference between the diffusive convection scheme and no convection scheme. Panels (c), (f) and (i) show the concentration difference between the Lagrangian convection scheme and no convection scheme.

northern South America and central Africa, as well the continental regions of North America and Eurasia.

5. COMPARISON WITH OBSERVATIONS

To assess the performance of the vertical redistribution by the convection scheme we have compared our models against measurements of vertical profiles and surface concentrations of ^{222}Rn . Figure 5 shows comparisons of modelled ^{222}Rn against summertime continental profiles compiled by Liu *et al.* (1984). The three model convection schemes are the same as described in section 4. This figure suggests that the new scheme gives the best agreement with the observations, particularly when comparing against 'C'-shaped radon profiles. The Lagrangian scheme is the only one that is able to simulate high radon concentrations around 8–12 km. This height range is typical of the outflow regions of summertime continental convective clouds. It must be remembered that the model values are averages over one month, whereas the measurements over America are single aircraft flights and those over the Ukraine are an average of five aircraft flights. While the model values are averages over all times of day, the flights generally occurred in the daytime when convective activity is stronger.

Measurements over coastal regions show less clear-cut results. Figure 6 compares the model against an average of 11 aircraft profiles over San Francisco (Kritz *et al.* 1998) and eight profiles over Nova Scotia (Zaucker *et al.* 1996). These regions are difficult to model as there are large gradients in ^{222}Rn concentration from the low values over the oceans to the high values over the land. The observed concentrations will depend strongly on the actual wind directions and strengths at the time of measurement, whereas the modelled values will more reflect the prevailing wind conditions. With predominantly westerly winds at these latitudes the west-coast site might be expected to be influenced by more maritime air and the east-coast site by more continental air. This is confirmed both in the observations and model calculations which show higher ^{222}Rn concentrations over Nova Scotia than over San Francisco, even though the region covered by the Nova Scotia measurements is mostly sea and the San Francisco region mostly land. At both sites the scheme without any convective transport fails to predict realistic concentrations above 4 km. The Lagrangian scheme shows smoother transitions than the diffusive one from the high boundary-layer concentrations to the lower free-troposphere concentrations. However, the gradients in the measured concentrations are much less, with boundary-layer values half those of the models and a more gradual transition towards the free-tropospheric values. If the aircraft profiles can be considered representative of the monthly and regional averages, then this could suggest that the model has insufficient venting of the boundary layer in these coastal regions. One obvious problem with simulating coastal measurements is the resolution of the model. For example the grid square holding the emissions for the San Francisco area extends out to 125°W . Measurements taken in the boundary layer will tend to be of marine air with slight contamination from local radon sources. In the model, boundary-layer air arriving at San Francisco will have started to pick up emissions from 125°W , about 250 km out to sea. Even though the emissions from the coastal grid square will only be about a half of those from a continental grid square, the air will still appear more polluted. Around Nova Scotia, most of the boundary-layer measurements were made over the sea. Although these will be strongly influenced by outflow from the continent, they receive no direct radon emission, unlike the model where radon is emitted over the entire area.

Only the Nova Scotia measurements show a 'C'-shaped profile characteristic of continental convection. None of the model profiles match this. The diffusive scheme has too sharp a transition at 2 km, although it agrees with the observations at 5–6 km. The

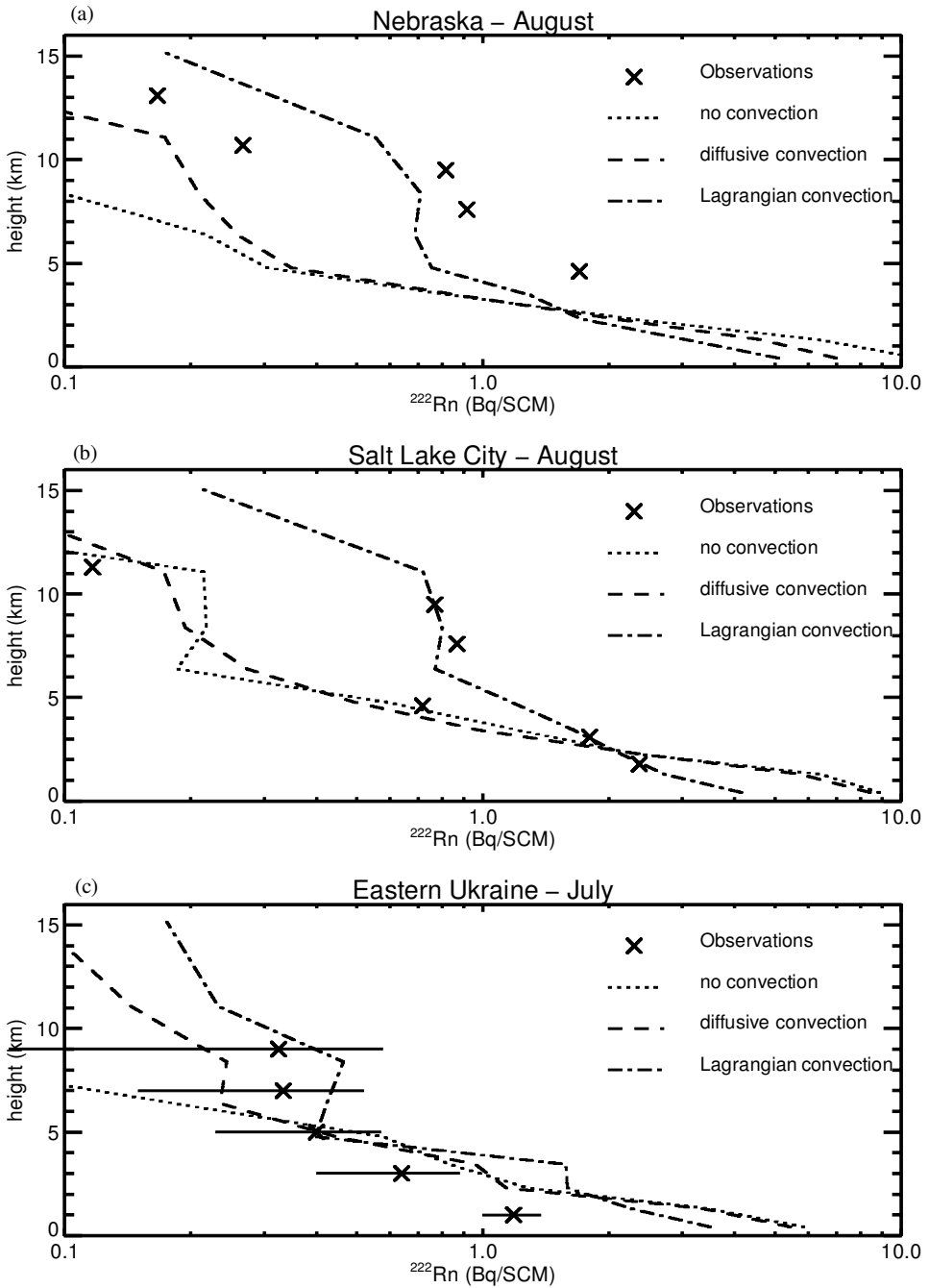


Figure 5. Comparison of modelled ^{222}Rn against observed continental summertime profiles over (a) Nebraska, (b) Salt Lake City, and (c) eastern Ukraine. The observations over the Ukraine are the means and standard deviations of measurements taken over five flights.

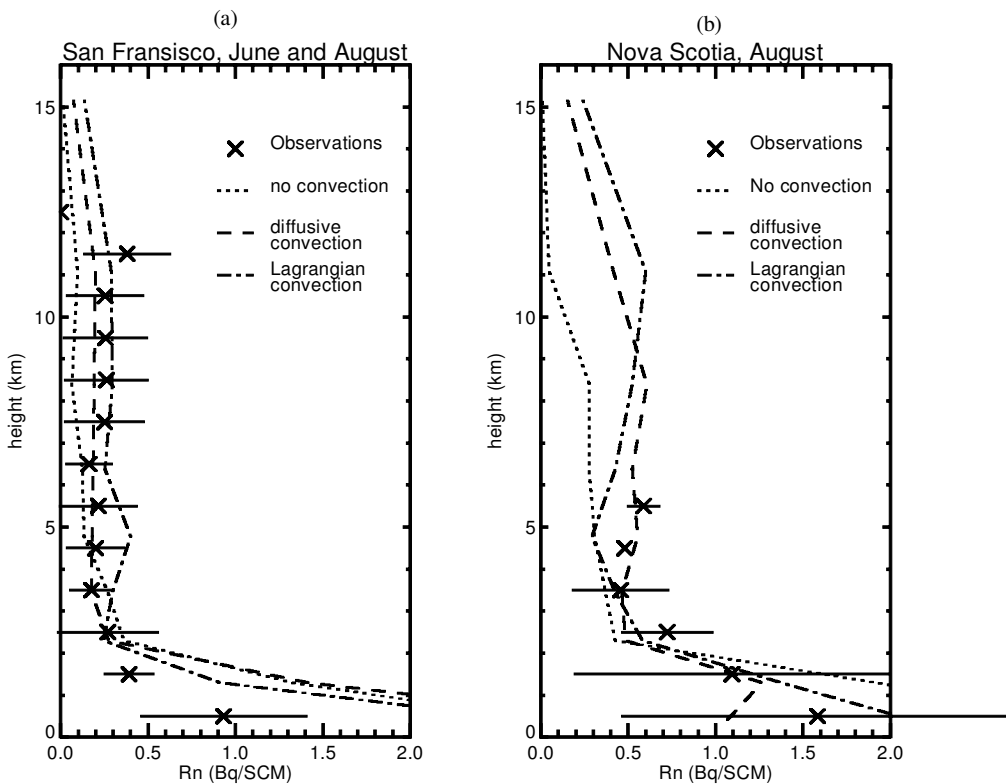


Figure 6. Comparison of modelled profiles of ^{222}Rn for the three convection schemes (see text) against observed coastal profiles: (a) the average of 11 profiles over San Francisco, and (b) the average of eight profiles over Nova Scotia.

Lagrangian scheme does have a 'C' shape, but the radon minimum occurs at too high an altitude, at 5 km. Neither the observations over San Francisco nor those over Nova Scotia are able to discriminate between the two different parametrizations of convection, although they do suggest the scheme with no convective transport is less realistic.

Surface ^{222}Rn data from two stations have been described by Hutter *et al.* (1995)*. Data for Mauna Loa and Bermuda are shown in Fig. 7. The concentrations are presented as monthly averages for the years 1991–1996 inclusive. Following Dentener *et al.* (1999), Mauna Loa data have been filtered to select only measurements taken between midnight and 0700 local time. This is to reduce the effect of local contamination due to upslope airflow. Interestingly, at the height of the Mauna Loa observatory (3400 m) there is little variation in the ^{222}Rn concentrations predicted by the different convection schemes, suggesting that the transport to Hawaii is dominated by large-scale advection rather than subgrid-scale convection. However, the modelled vertical profiles over Mauna Loa (not shown) do indicate some differences. In particular, compared with the other two schemes, the scheme with no convective transport generally has higher surface concentrations and lower free-tropospheric concentrations. All the modelled concentrations underestimate the Mauna Loa observations in the spring, a problem that is common to many other chemistry-transport models (Dentener *et al.* 1999; Brasseur *et al.* 1996; Jacob *et al.* 1997). Dentener *et al.* (1999) suggested that the high observed

* These data are available on-line at <http://www.eml.doe.gov>

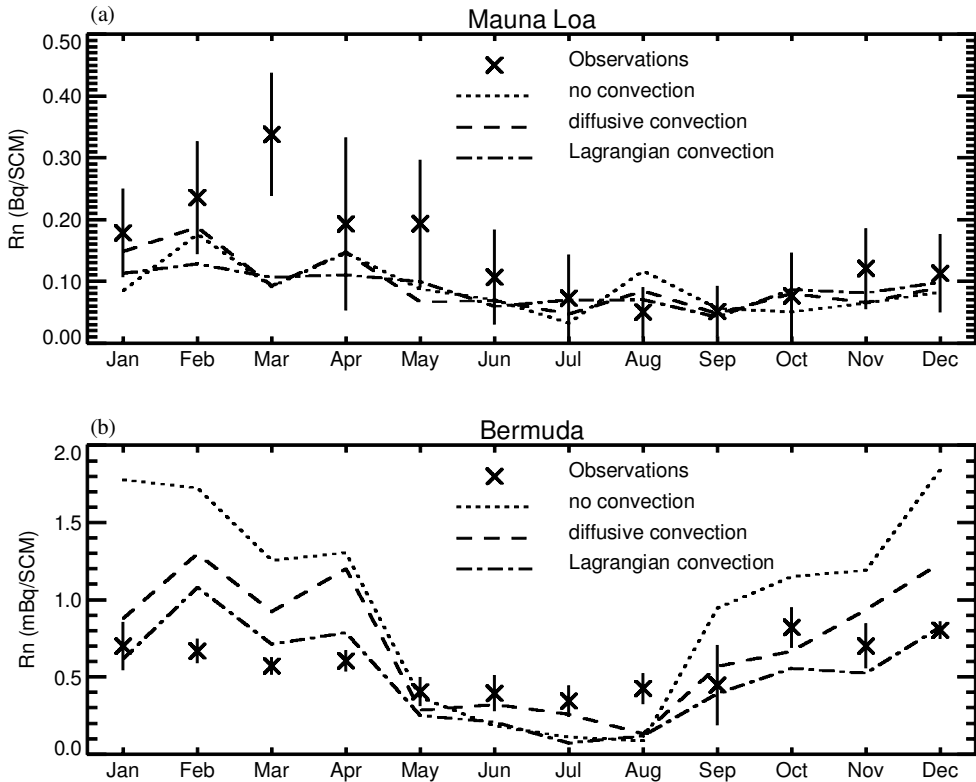


Figure 7. Comparison of the time-series of monthly averaged modelled ^{222}Rn values at the surface for the three convection schemes (see text) against observed marine data: (a) Mauna Loa (concentrations are for 3.4 km above sea level) and (b) Bermuda (concentrations are for approximately sea level).

concentrations may be due to vigorous convection over east Asia transporting radon up to the level of the strong westerly winds. Our results seem to imply that convection is less important, since there is little difference in the modelled concentrations whether or not any convective transport is simulated. The transport from east Asia to Mauna Loa is critically dependent on the location of the Pacific anticyclone (Brasseur *et al.* 1996). If the anticyclone simulated by the climate GCM is further to the east or north than the actual meteorology at the time the measurements were taken, then the modelled ^{222}Rn will be more characteristic of the central Pacific than east Asia, relative to the measurements. This will result in the model underestimating the Mauna Loa ^{222}Rn concentrations and being less sensitive to continental convection.

In contrast to the Mauna Loa site, the modelled ^{222}Rn concentrations at Bermuda vary strongly according to the convection scheme used. This is particularly true in the winter half of the year when Bermuda is predominantly influenced by westerly winds bringing radon from eastern North America. Bermuda is only around 1000 km from the continental USA, and so receives radon directly from the continental boundary layer. The effect of this can be seen when comparing the different model convection schemes. With no convective transport the continental boundary layer is less ventilated than with the other schemes and, hence, higher concentrations of ^{222}Rn build up and, in winter (September to April), are advected over to Bermuda. The Lagrangian scheme in this case ventilates the boundary layer more efficiently than the diffusive scheme because the

entrainment into the convective column in the Lagrangian scheme peaks below the cloud base rather than being constant with height as in the diffusive scheme. To compare the model with the observations, measurements taken during the night are excluded as ^{222}Rn concentrations are elevated in the nocturnal boundary layer due to local emissions. This is particularly noticeable during anticyclonic conditions in the summer months when Bermuda is influenced by the Azores high. The chemistry-transport model is not able to resolve emissions from an area as small as Bermuda. In the spring, the model's schemes all overestimate the radon concentrations, with the Lagrangian scheme giving the closest results to the observations. This overestimate has been noticed with other chemistry-transport models (Dentener *et al.* 1999; Mahowald *et al.* 1997). In the summer, both the no-convection and Lagrangian convection schemes underestimate the radon concentrations. During this season Bermuda receives air masses that have circulated around the Azores high and hence are depleted in ^{222}Rn . The diffusive convection scheme predicts greater concentrations and so agrees better with the observations. The greater concentrations are due to bringing down air from higher altitudes where there is more transport from North America than at the surface. This effect is larger using the diffusive convection scheme since, in this scheme, the boundary-layer air is uniformly redistributed with height over the continent by a convective event. Over Bermuda, convection can mix air from upper levels down to the surface in one time step. This contrasts with the Lagrangian scheme where boundary-layer air is transported preferentially to the altitude of convective outflow (10–15 km) over the continent. Over Bermuda, any subsidence in the Lagrangian scheme due to convective events will bring down air from the upper troposphere too slowly for the elevated ^{222}Rn to be observed at the surface. We have not filtered Bermuda data according to wind direction or speed and, therefore, some of the higher summertime observations may be influenced by local emissions.

6. CONCLUSIONS

We have shown that the parametrization of convective-transport processes has a significant effect on the three-dimensional distribution of ^{222}Rn predicted by a global chemical-transport model. In particular, the addition of convective-transport parametrizations reduces the predicted surface concentrations of ^{222}Rn over the continents and increases the predicted concentrations in the free troposphere.

The comparison between model simulations and observations shows that having no convective transport is unrealistic, as the model predicts a decrease in ^{222}Rn concentration between the continental boundary layer and the free troposphere that is too large. The Lagrangian parametrization gives a greater venting of the boundary layer than the diffusive scheme and preferentially detrains this in the mid to upper troposphere. However, surface ^{222}Rn concentrations are often still too high, even with the Lagrangian scheme. Over the continents in summertime, the Lagrangian scheme gives very good agreement with the observed 'C'-shaped vertical ^{222}Rn profiles, a feature that the previous diffusive convective transport scheme was not able to simulate. Summertime convection over large continents is generally strong and deep, giving a clear convective signal in the radon profiles. Over coastal regions and island sites the radon profiles are affected by other transport processes as well as by convection. Comparisons between predicted and measured ^{222}Rn in these locations are not able to conclude whether one convection scheme is better than the other.

In this paper we have focused on the simulations of ^{222}Rn distributions, as this species has the simplest chemistry and allows the effects of the parametrization of

convective transport to be seen most clearly. It should be remembered that ^{222}Rn is only used to test the convection schemes. From the chemical point of view, it is the ability of the model to convectively transport reactive species (such as NO_x , ozone and volatile organic compounds) that is most important.

ACKNOWLEDGEMENTS

This study was supported as part of the Public Meteorological Service R&D programme of the Met Office and by the Department of the Environment, Transport and the Regions through contracts PECD 7/12/37 (Global Atmosphere Division) and EPG 1/3/143 (Air and Environmental Quality Division).

REFERENCES

- Berntsen, T. K. and Isakesen, I. S. A. 1997 A global three-dimensional chemical transport model for the troposphere. I. Model description and CO and ozone results. *J. Geophys. Res.*, **102**, 21239–21280
- Brasseur, G. P., Hauglustaine, D. A. and Walters, S. 1996 Chemical compounds in the remote Pacific troposphere: Comparison between MLOPEX measurements and chemical transport model calculations. *J. Geophys. Res.*, **101**, 14795–14813
- Chock, D. P. and Winkler, S. L. 1994 A comparison of advection algorithms coupled with chemistry. *Atmos. Environ.*, **28**, 2659–2675
- Collins, W. J., Stevenson, D. S., Johnson, C. E. and Derwent, R. G. 1997 Tropospheric ozone in a global-scale three-dimensional Lagrangian model and its response to NO_x emission controls. *J. Atmos. Chem.*, **26**, 223–274
- 1999 Role of convection in determining the budget of odd hydrogen in the upper troposphere. *J. Geophys. Res.*, **104**, 26927–26941
- Cullen, M. J. P. 1993 The unified forecast/climate model. *Meteorol. Mag.*, **122**, 81–94
- Dabdub, D. and Seinfeld, J. H. 1994 Numerical advective schemes used in air quality models—sequential and parallel implementation. *Atmos. Environ.*, **28**, 3369–3385
- Dentener, F., Feichter, J. and Jeuken, A. 1999 Simulation of the transport of Rn^{222} using on-line and off-line global models at different horizontal resolutions: A detailed comparison with measurements. *Tellus*, **51B**, 573–602
- Doty, K. G. and Perkey, D. J. 1993 Sensitivity of trajectory calculations to the temporal frequency of wind data. *Mon. Weather Rev.*, **121**, 387–401.
- Gidel, L. T. 1983 Cumulus cloud transport of transient tracers. *J. Geophys. Res.*, **88**, 6587–6599
- Gregory, D., Kershaw, R. and Inness, P. M. 1997 Parametrization of momentum transport by convection. II: Tests in single-column and general circulation models. *Q. J. R. Meteorol. Soc.*, **123**, 1153–1183
- Hutter, A. R., Larsen, R. J., Martin, H. and Merrill, J. T. 1995 Radon-222 at Bermuda and Mauna Loa: Local and distant sources. *J. Radiometr. Nuclear Chem.*, **193**, 309–318
- Jacob, D. J. and Prather, M. J. 1990 Radon-222 as a test of convective transport in a general circulation model. *Tellus*, **42B**, 118–134
- Jacob, D. J., Prather, M. J., Rasch, P. J., Shia, R.-L., Balkanski, Y. J., Beagley, S. R., Bergmann, D. J., Blacksher, W. T., Brown, M., Chiba, M., Chipperfield, M. P., de Grandpré, J., Dignon, J. E., Feichter, J., Genthon, C., Grose, W. L., Kasibhatla, P. S., Köhler, I., Kritz, M. A., Law, K., Penner, J. E., Ramonet, M., Reeves, C. E., Rouanet, D. A., Stockwell, D. Z., van Velthoven, P. F. J., Verver, G., Wild, O., Yang H. and Zimmerman, P. 1997 Evaluation and intercomparison of global atmospheric transport models using ^{222}Rn and other short-lived tracers. *J. Geophys. Res.*, **102**, 5953–5970

- Jaeglé, L., Jacob, D. J., Wennberg, P. O., Spivakovsky, C. M., Hanisco, T. F., Lanzendorf, E. L., Hints, E. J., Fahey, D. W., Keim, E. R., Proffitt, M. H., Atlas, E., Flocke, F., Schauffler, S., McElroy, C. T., Midwinter, C., Pfister, L. and Wilson, J. C. 1997 Observed OH and HO₂ in the upper troposphere suggest a major source from convective injection of peroxides. *Geophys. Res. Lett.*, **24**, 3181–3184
- Johns, T. C., Carnell, R. E., Crossley, J. F., Gregory, J. M., Mitchell, J. F. B., Senior, C. A., Tett, S. F. B. and Wood, R. A. 1997 The second Hadley Centre coupled ocean–atmosphere GCM: Model description, spinup and validation. *Climate Dyn.*, **13**, 103–134
- Kanakidou, M., Dentener, F. J., Brasseur, G. P., Collins, W. J., Bernsten, T. K., Hauglustaine, D. A., Houweling, S., Isaksen, I. S. A., Krol, M., Lawrence, M. G., Muller, J. F., Poisson, N., Roelofs, G. J., Wang, Y. and Wauben, W. M. F. 1999a 3-D global simulations of tropospheric CO distributions—results of the GIM/IGAC intercomparison 1997 exercise. *Chemosphere: Global Change Science*, **1**, 263–282
- Kanakidou, M., Dentener, F. J., Brasseur, G. P., Collins, W. J., Bernsten, T. K., Hauglustaine, D. A., Houweling, S., Isaksen, I. S. A., Krol, M., Law, K. S., Lawrence, M. G., Muller, J. F., Plantevin, P. H., Poisson, N., Roelofs, G. J., Wang, Y. and Wauben, W. M. F. 1999b '3-D global simulations of tropospheric chemistry with focus on ozone distributions—results of the GIM/IGAC intercomparison 1997 exercise'. European Commission report EUR18842, Brussels
- Kritz, M. A., Rosner, S. W. and Stockwell, D. Z. 1998 Validation of an off-line three-dimensional chemical transport model using observed radon profiles. 1. Observations. *J. Geophys. Res.*, **103**, 8425–8432
- Lacis, A. A., Weubbles, D. J. and Logan, J. A. 1990 Radiative forcing of climate by changes in the vertical distribution of ozone. *J. Geophys. Res.*, **95**, 9971–9981
- Lawrence, M. G., Crutzen, P. J., Rasch, P. J., Easton, B. E. and Mahowald, N. M. 1999 A model for studies of tropospheric photochemistry: Description, global distributions, and evaluation. *J. Geophys. Res.*, **104**, 26245–26277
- Lee, T.-Y., Park, S.-W. and Kim, S.-B. 1997 Dependence of trajectory accuracy on the spatial and temporal densities of wind data. *Tellus*, **49B**, 199–215
- Lin, X., Trainer, M. and Liu, S. C. 1988 On the nonlinearity of the tropospheric ozone production. *J. Geophys. Res.*, **93**, 15879–15888
- Liu, S. C., McAfee, J. R. and Cicerone, R. J. 1984 Radon 222 and tropospheric vertical transport. *J. Geophys. Res.*, **89**, 7291–7297
- Madronich, S. 1987 Photodissociation in the atmosphere. 1. Actinic flux and the effects of ground reflections and clouds. *J. Geophys. Res.*, **92**, 9740–9752
- Mahowald, N. M., Rasch, P. J., Easton, B. E., Whittlestone, S. and Prinn, R. G. 1997 Transport of ²²²radon to the remote troposphere using the model of atmospheric transport and chemistry and assimilated winds from ECMWF and the National Centers for Environmental Prediction/NCAR. *J. Geophys. Res.*, **102**, 28139–28151
- Mari, C., Jacob, D. J. and Bechtold, P. 2000 Transport and scavenging of soluble gases in a deep convective cloud. *J. Geophys. Res.*, **105**, 22255–22267
- Methven, J. 1997 'Offline trajectories: Calculation and accuracy'. UGAMP Technical Report 44, Department of Meteorology, Reading University, Reading, UK

- Penner, J. E., Bergmann, D. J., Walton, J. J., Kinnison, D., Prather, M. J., Rotman, D., Price, C., Pickering, K. E. and Baughcum, S. L. 1998 An evaluation of upper troposphere NO_x with two models. *J. Geophys. Res.*, **103**, 22097–22113
- Pickering, K. E., Thompson, A. M., Scala, J. R., Tao, W.-K. and Simpson, J. 1992 Ozone production potential following convective redistribution of biomass burning emissions. *J. Atmos. Chem.*, **14**, 297–313
- Prather, M. J. and Jacob, D. J. 1997 A persistent imbalance in HO_x and NO_x photochemistry of the upper troposphere driven by deep tropical convection. *Geophys. Res. Lett.*, **24**, 3189–3192
- Price, C., Penner, J. and Prather, M. 1997 NO_x from lightning. 1. Global distribution based on lightning physics. *J. Geophys. Res.*, **102**, 5929–5941
- Rasch, P. J., Feichter, J., Law, K., Mahowald, N., Penner, J., Benkovitz, C., Genthon, C., Giannakopoulos, C., Kasibhatla, P., Koch, D., Levy, H., Maki, T., Prather, M., Roberts, D. L., Roelofs, G.-J., Stevenson, D., Stockwell, Z., Taguchi, S., Kritz, M., Chipperfield, M., Baldocchi, D., McMurry, P., Barrie, L., Balkanski, Y., Chatfield, R., Kjellstrom, E., Lawrence, M., Lee, H. N., Lelieveld, J., Noone, K. J., Seinfeld, J., Stenchikov, G., Schwartz, S., Walcek, C. and Williamson, D. 2000 A comparison of scavenging and deposition processes in global models: Results from the WCRP Cambridge Workshop of 1995. *Tellus*, **52B**, 1025–1056
- Smith, R. N. B. 1990 A scheme for predicting layer clouds and their water contents in a general circulation model. *Q. J. R. Meteorol. Soc.*, **116**, 435–460
- Stevenson, D. S., Johnson, C. E., Collins, W. J. and Derwent, R. G. 1997 The impact of aircraft nitrogen oxide emissions on tropospheric ozone studied with a 3-D Lagrangian model including fully diurnal chemistry. *Atmos. Environ.*, **31**, 1837–1850
- Stevenson, D. S., Collins, W. J., Johnson, C. E. and Derwent, R. G. 1998a Intercomparison and evaluation of atmospheric transport in a Lagrangian model (STOCHEM), and an Eulerian model (UM), using ^{222}Rn as a short-lived tracer. *Q. J. R. Meteorol. Soc.*, **125**, 2477–2493
- Stevenson, D. S., Collins, W. J., Johnson, C. E., Derwent, R. G., Shine, K. P. and Edwards, J. M. 1998b Evolution of tropospheric ozone radiative forcing. *Geophys. Res. Lett.*, **25**, 3819–3822
- Thompson, A. M., Pickering, K. E., Dickerson, R. R., Ellis Jr., W. G., Jacob, D. J., Scala, J. R., Tao, W.-K., McNamara, D. P. and Simpson, J. 1994 Convective transport over the central United States and its role in regional CO and ozone budgets. *J. Geophys. Res.*, **99**, 18703–18711
- Thuburn, J. and McIntyre, M. E. 1997 Numerical advection schemes, cross-isentropic random walks, and correlations between chemical species. *J. Geophys. Res.*, **102**, 6775–6797
- Walton, J. J., MacCracken, M. C. and Ghan, S. J. 1988 A global-scale Lagrangian trace species model of transport, transformation, and removal processes. *J. Geophys. Res.*, **93**, 8339–8354
- Zaucker, F., Daum, P. H., Wetterauer, U., Berkowitz, C., Kromer, B. and Broecker, W. S. 1996 Atmospheric ^{222}Rn measurements during the 1993 NARE Intensive. *J. Geophys. Res.*, **101**, 29149–29164